

# Sinonasal Anatomy



Sanjay Vaid, MD (Radiology)<sup>a,\*</sup>, Neelam Vaid, MS, DNB (ENT)<sup>b</sup>

## KEYWORDS

- Nasal cavity • Paranasal sinuses (PNSs) • Anatomy • Anatomic variants
- Computed tomography (CT)

## KEY POINTS

- The radiologist needs to be familiar with the imaging anatomy as visualized by an endoscopic sinus surgeon.
- Multiplanar region-specific reporting and preoperative identification of anatomic variants provide the endoscopic surgeon with a useful intraoperative roadmap and avoid intraoperative complications.
- This article reviews the imaging anatomy of the nasal cavity and paranasal sinuses and discusses the clinical relevance of the anatomic variants in the sinonasal region.

 Video content accompanies this article at <http://www.neuroimaging.theclinics.com>.

## INTRODUCTION

Anatomic concepts of the paranasal sinuses (PNSs) have been known since the late nineteenth and early twentieth centuries.<sup>1</sup> This article reviews the embryology of the PNSs and mentions, in brief, the computed tomography (CT) and MR imaging techniques for imaging this region. CT is the imaging modality of choice for identifying key anatomic features and anatomic variants of the nasal cavity and PNSs.

### *Imaging Techniques and Protocol*

All CT examinations are performed on a multi-channel CT scanner and viewed on a workstation to facilitate multiplanar reconstructions in standard orthogonal and nonorthogonal planes. This enables image reconstruction at a submillimeter level (up to 0.34 mms). CT studies should be viewed in all 3 orthogonal planes for optimal visualization of anatomic structures. Three different window level and window width settings should be used for viewing the CT images (PNS, bone, and brain settings) to avoid missing or

misinterpreting important findings (**Fig. 1**). Customized low-dose CT protocols are used while scanning the pediatric population.<sup>2</sup> Use of cone-beam CT is advised, if available, to minimize radiation dose in children and young adults.<sup>3,4</sup> Contrast-enhanced CT or MR imaging examinations are indicated for evaluating intracranial, intra-orbital, and nasopharyngeal complications.<sup>5</sup>

### *Embryology*

The embryo develops its first identifiable head and face between the fourth and fifth weeks of gestational age with a central orifice called the stomodeum, which is surrounded by the mandibular, maxillary, and frontonasal prominences. The ethmoid sinuses are present at birth, whereas the other sinuses (frontal, maxillary, and sphenoid) develop owing to pneumatization beyond the confines of the olfactory capsule. Hence the ethmoid sinus is phylogenetically, anatomically, embryologically, and functionally different from the other air-containing PNSs.<sup>6</sup> The further ossification pattern is complex and the reader is referred to numerous excellent texts in the literature for a

<sup>a</sup> Head Neck Imaging Division, Star Imaging and Research Center, Connaught Place (ground floor), Bund Garden Road, Pune 411001, Maharashtra, India; <sup>b</sup> Department of Otorhinolaryngology, K.E.M. Hospital, 489 Rasta Peth, Pune 411001, Maharashtra, India

\* Corresponding author.

E-mail address: [svaidhn@gmail.com](mailto:svaidhn@gmail.com)

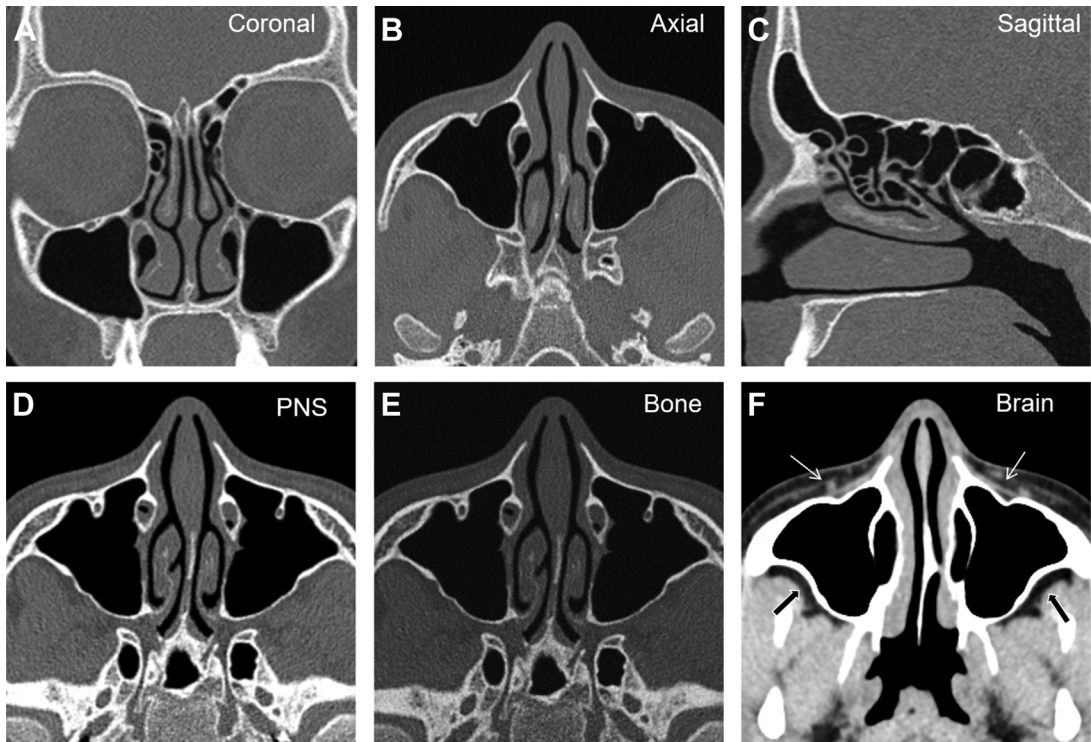


**Fig. 1.** Viewing planes and window settings for paranasal CT scans. Axial (A), Coronal (B), and sagittal (C) planes for optimal viewing anatomy of the PNSs. Axial CT images in paranasal sinus (D), bone (E), and brain (F) windows showing premaxillary (white arrows) and retro-antral (black arrows) regions.

more detailed discussion. The pneumatization pattern is unique to each group of sinuses and the continuous change in the size and aeration of the sinus as the child grows has a significant impact on the treatment/surgery of sinus pathologic condition in the pediatric age group.<sup>7</sup> **Table 1** outlines the growth pattern of each sinus group and the ostiomeatal complex with the resultant clinical implications. **Fig. 2** depicts the childhood development of the PNSs and related structures.

### Anatomy Overview of the Sinonasal Region

1. Anterior sinonasal region
  - Nasal cavity: nasal valves, nasal septum, nasal turbinates, and meatuses.
  - Uncinate process.
  - Frontal sinus and the frontal sinus drainage pathway (FSDP) anatomy.
  - Anterior ethmoid sinuses and lamellar anatomy.
  - Maxillary sinus and the ostiomeatal complex.
2. Posterior sinonasal region
  - Posterior sinus group: posterior ethmoid sinus and the sphenoid sinus.
3. Shared anatomic interfaces with adjacent structures

- Anterior skull base: the olfactory fossa and the ethmoidal skull base.
- Lamina papyracea and the anterior ethmoidal artery (AEA).

### The Nasal Cavity

The nasal cavities are triangular structures separated by the nasal septum in the midline, limited superiorly by the cribriform plate and inferiorly by the hard palate.

### The nasal cycle

The mucosal lining over the nasal septum and the nasal turbinates is influenced by the nasal cycle, which is responsible for alternating changes in the turbinate sizes owing to mucosal engorgement.<sup>8</sup> This cyclical and physiologic enlargement of the turbinates alternates between both nasal cavities every 45 minutes to an hour and should not be mistaken for pathologic condition.

### The nasal valves

Most texts discussing nasal cavity imaging anatomy tend to concentrate on the bony posterior three-fourth portion, that is, the nasal septum, septal spurs, and nasal turbinates. The anterior one-fourth is an important but frequently

**Table 1**  
**Pneumatization/ossification pattern of paranasal sinuses and related structures**

Sr.no	Sinus/Structure	Childhood Development	Clinical Implications
1.	Frontal sinus	<p>Not seen on imaging at birth.  Present as a small pit or furrow at birth</p> <p>Slow pneumatization between 1 and 4 y, rapid growth between 4 and 8 y, reaching the orbital roof by 5–7 y of age and attaining adult appearance by 12 y of age</p> <p>Narrower antero-posterior diameter as compared with the adult</p>	<p>Children cannot develop frontal sinusitis before 4 y of age</p> <p>Frontal trephination procedures are contraindicated in an immature frontal sinus (till it reaches the orbital plate) due to the risk of inadvertent intracranial penetration, meningeal trauma, and likely iatrogenic infection</p>
2.	Ethmoid sinus	<p>Present and seen on imaging at birth</p> <p>Rapid pneumatization between 1 and 4 y</p> <p>Slow growth between 4 and 8 y</p> <p>Adult appearance by 12 y of age</p>	<p>Source of sinus/contiguous orbital infection in young children</p> <p>Accessible to both internal and external drainage procedures if required</p>
3.	Maxillary sinus	<p>Not seen on imaging at birth.  Present as a shallow rounded sac at birth</p> <p>Rapid pneumatization between 1 and 4 y: floor of the sinus reaches level of the inferior meatus by 7 y of age</p> <p>Adult appearance is attained by 12–14 y when the floor of the sinus reaches level of the nasal cavity floor</p> <p>Slow pneumatization continues till 20 y of age</p>	<p>Height discrepancy between the inferior margins of the sinus and the nasal cavity precludes the use of certain surgical techniques in children. These procedures may damage developing teeth, cause inadvertent injury to lateral sinus wall, or may be ineffective in treating the pathologic condition completely</p>
4.	Sphenoid sinus	<p>Not seen on imaging at birth. Tiny mucosal sac posterior to the nasal capsule at birth</p> <p>Pneumatizes between 1 and 3 y of age. Grows progressively between 7 and 14 y and may continue to pneumatize further into adulthood</p>	<p>Limited clinical significance before the age of 10 y</p> <p>As the posterior ethmoid sinus pneumatizes earlier, it can grow above the developing sphenoid sinus to form the Onodi cell.</p> <p>Location of critical neurovascular structures around the sphenoid sinus depends on the degree of pneumatization of the sinus</p>
5.	The ostiomeatal complex	<p>All components are developed and present in the newborn</p>	<p>All the components of the ostiomeatal complex are packed tightly together leading to a narrow caliber of the infundibulum, which must be appreciated preoperatively.</p> <p>Proximity of the uncinate osseous to the lamina papyracea predisposes to inadvertent intraorbital penetration</p>
6.	Anterior cranial fossa	<p>The midline structures (crista galli, cribriform plates, and perpendicular ethmoid plate) are cartilaginous at birth and ossify by 2 y of age. They represent the “lucent stripe” on CT scans of infants because the surrounding ethmoid bone, vomer, and palate are ossified</p>	<p>The “lucent stripe” should not be misinterpreted as a bony defect, sinus tract, cephalocele, or bony destruction</p>

From Vaid S, Vaid N. Normal Anatomy and Anatomic Variants of the Paranasal Sinuses on Computed Tomography. *Neuroimaging Clin N Am.* 2015 Nov;25(4):527 to 48.

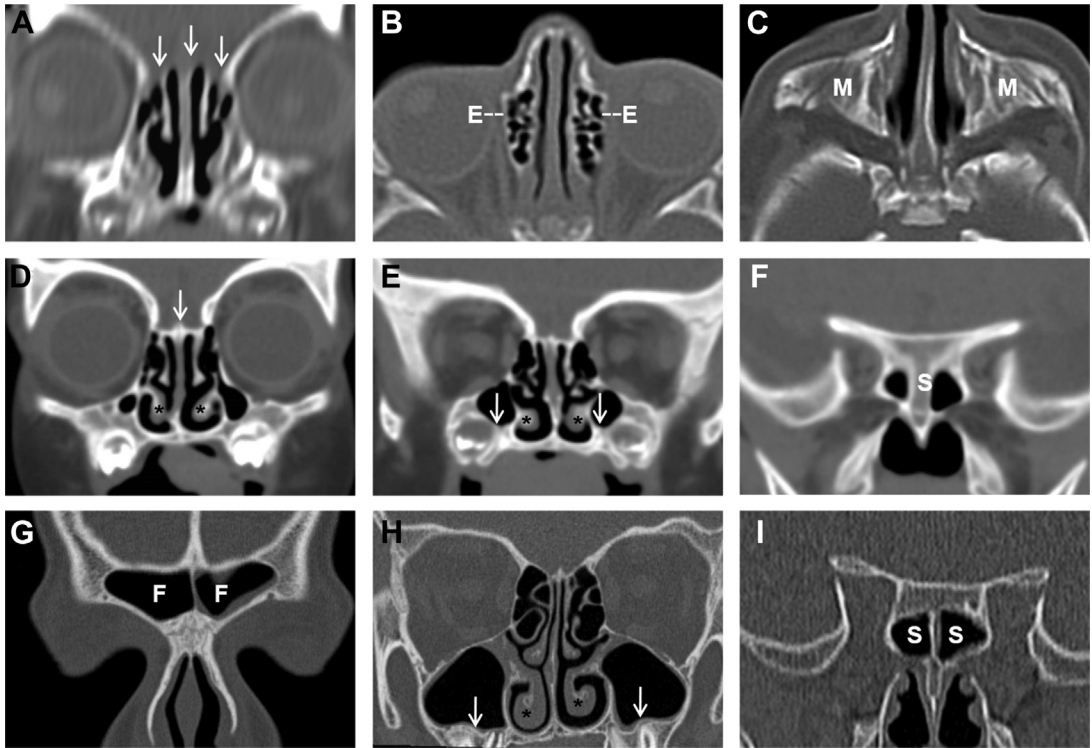


**Fig. 2.** Paranasal sinus development. At birth (A–C): (A) Unossified central anterior skull base structures resulting in “lucent stripes” (arrows), (B) pneumatized ethmoidal labyrinth (E), (C) M: nonpneumatized maxillary sinuses. At 1 year (D–F): (D) Anterior skull base ossification (arrow) is complete. (E) Partially pneumatized maxillary sinus floor (arrows) to level of inferior turbinates (\*). (F) Early sphenoid sinus (S) pneumatization. At 5 years (G–I): (G) Frontal sinus (F) pneumatized to the orbital roof. (H) Maxillary sinus floor (arrows) to level of the inferior meatus. (I) Progressive sphenoid sinus pneumatization. (From Vaid S, Vaid N. Normal Anatomy and Anatomic Variants of the Paranasal Sinuses on Computed Tomography. *Neuroimaging Clin N Am.* 2015 Nov;25(4):527 to 48.)

neglected anatomic area comprising the external nasal valves (ENVs) and internal nasal valves (INVs) with intervening nasal vestibule (Fig. 3). The ENV is formed by the columella, the nasal floor, and the nasal rim. The INV is the narrowest region in the anterior nose formed by the nasal septum, the upper lateral nasal cartilage, head of the inferior turbinate, and the pyriform aperture soft tissues<sup>9</sup> (see Fig. 3). The cross-sectional area and angle of the INV are measured in a standardized coronal image, anterior to the head of the inferior turbinate (see Fig. 3). The normal range for the INV angle ranges from 10° to 15°,<sup>9</sup> and INV areas range from 0.47 to 0.51 cm<sup>2</sup>. An INV having an area of less than 0.30 cm<sup>2</sup> on CT suggests the presence of clinically significant nasal airway obstruction.<sup>10</sup>

### The nasal septum

The nasal septum consists of an anterior cartilaginous component (the septal cartilage) and a posterior bony component (the bony septum)

comprising of the vomer and the perpendicular plate of the ethmoid.<sup>11</sup>

### Anatomic Variations

- (Fig. 4) 1. Septal deviation: Seen in 20% to 79% of the population.<sup>12</sup> The septum is commonly deviated in its inferior portion near the chondro-vomer junction and can also assume an “S”-shaped configuration with deviation to both sides of the midline. Bony septal spurs may be associated with septal deviations and may form adhesions with the adjacent turbinates.
2. Septal pneumatization: Pneumatization can occur anteriorly from the crista galli or posteriorly from the sphenoid sinus.

### The Nasal Turbinates and Meatuses (or Meati)

The lateral walls of the nasal cavities are complex structures that support the inferior, middle, and superior nasal turbinates, and occasionally, a fourth turbinate known as the supreme turbinate.

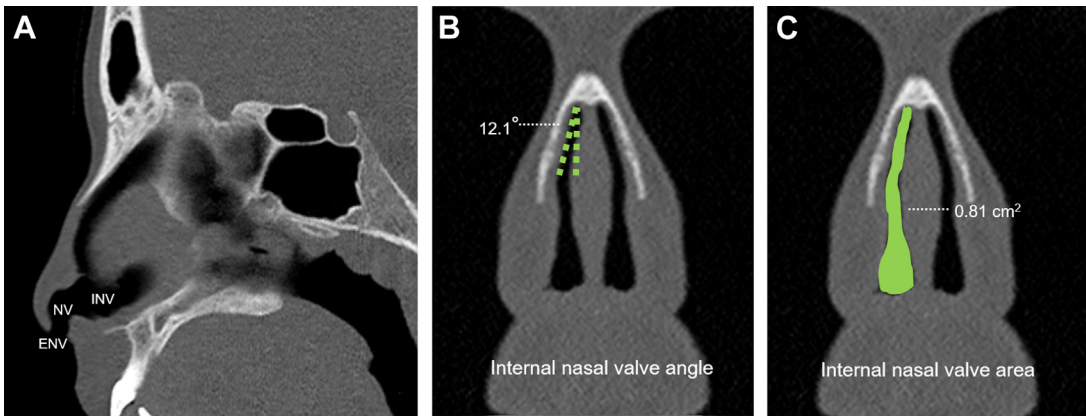


**Fig. 3.** Anatomy of the nasal valves. Parasagittal image (A) showing locations of the ENV and INV with intervening nasal vestibule (NV). Coronal CT images show measured angle (B) and measured area (C) for the INV.

These turbinates divide the nasal cavity into the superior, middle, and inferior meatuses (or meati) (Fig. 5). The superior meatus drains the posterior ethmoidal air cells and the sphenoid sinus through

the spheno-ethmoidal recess. The middle meatus drains the frontal sinus via the FSDP, the maxillary sinus via the maxillary ostium, and the anterior ethmoidal air cells. The inferior meatus drains the

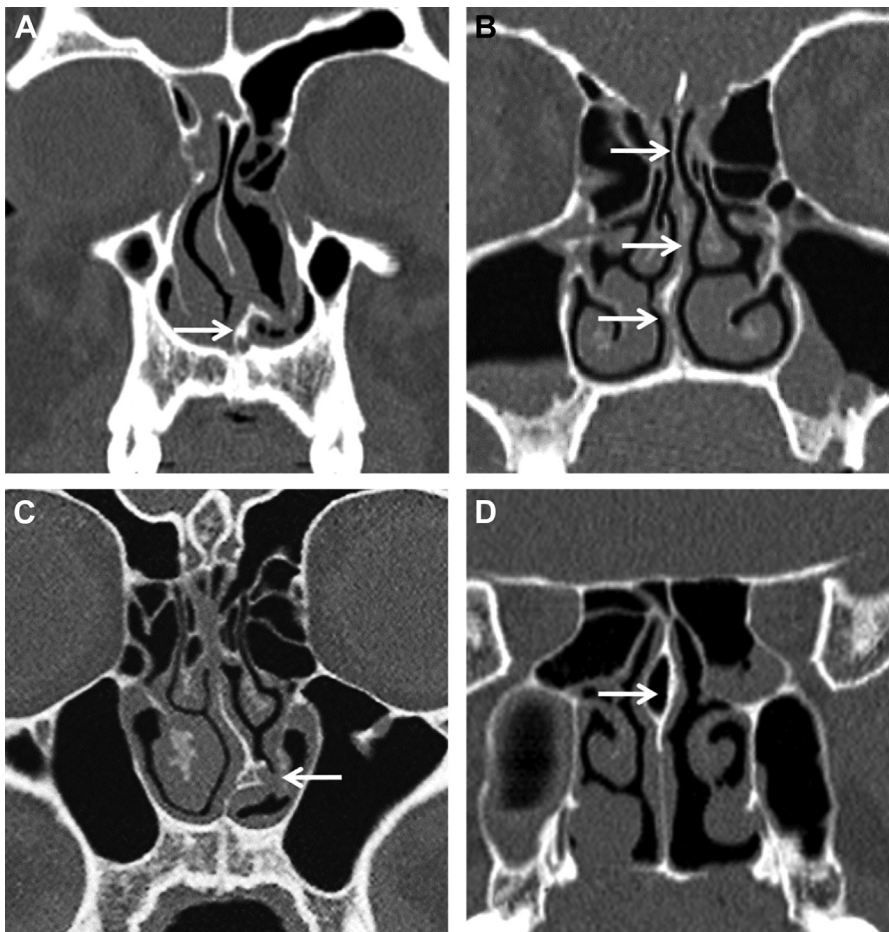


**Fig. 4.** Nasal septum variants. Coronal CT images showing nasal septum variants (arrows): (A) vomero-septal junction deviation, (B) S-shaped deviation, (C) bony septal spur with adhesion to inferior turbinate, and (D) posterior septal pneumatization.

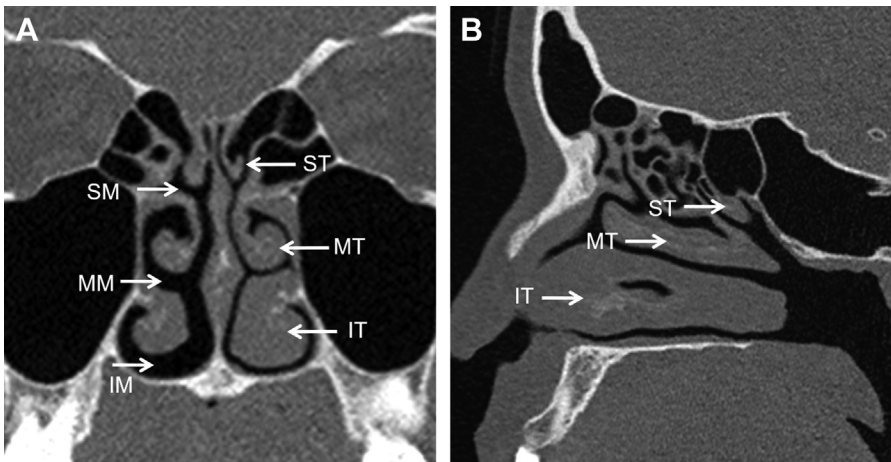


**Fig. 5.** Nasal turbinates and meatuses. Coronal (A) and parasagittal (B) images show inferior, middle, and superior nasal turbinates (IT, MT, ST) with corresponding inferior, middle, and superior nasal meatuses (IM, MM, SM).

nasolacrimal apparatus via the nasolacrimal duct.<sup>8</sup> The middle and inferior nasal turbinates usually have a similar shape exhibiting a convex margin medially and a concave margin laterally.

The middle turbinate is a part of the ethmoid bone with attachments in all 3 orthogonal planes.<sup>8</sup> The anterior part of the middle turbinate is oriented vertically, attaching superiorly to the anterior skull base at the lateral border of the cribriform plate. The posterior part attaches to the lamina papyracea and to the medial wall of the maxillary sinus (Video 1: Coronal CT depicting multiplanar attachments of the middle turbinate). The obliquely directed midportion of the middle turbinate is known as the basal lamella marking the division between the anterior and posterior ethmoidal sinuses.<sup>12</sup>

### Anatomic Variants

1. Concha bullosa: Pneumatization of the inferior bulbous portion of the middle turbinate occurs in approximately 24% to 55% of the population and is usually bilateral (Fig. 6).<sup>8</sup> If the pneumatization is restricted to the vertical lamella of the turbinate, above the level of the ostiomeatal unit, it is termed as an interlamellar cell of Grunwald, lamellar bulla, or a conchal neck air cell. Pneumatization of the middle turbinate has also been classified in the past as bulbous, lamellar, and extensive by Bolger and colleagues.<sup>13</sup> A new classification has been proposed by Calvo-Henríguez and colleagues<sup>14</sup> according to the degree of pneumatization of the vertical lamella of the middle turbinate.
2. Paradoxical middle turbinate: In 26% of the population, the middle turbinate exhibits a paradoxical lateral convexity (12).

3. Rare anatomic variants: Occasionally, the inferior portion of the middle turbinate curves acutely on itself producing a deep invagination called a turbinate sinus.<sup>8</sup> A bifid turbinate is formed when 2 bony lamellae share the same root.<sup>15</sup>
4. Pneumatized basal lamella may be mistaken for an anterior ethmoidal air cell leading to incomplete exploration of the posterior ethmoid sinuses.

### The Uncinate Process

The uncinat process is a thin crescent-shaped bone oriented in a sagittal oblique anterosuperior to a posteroinferior direction. Posteriorly the uncinat has a free concave margin. The superior attachment of the uncinat process may be variable. The ethmoidal infundibulum is located between the uncinat process and the inferomedial wall of the orbit.<sup>16</sup>

### Anatomic Variants

1. Variable superior attachments: The uncinat process may attach either to the lamina papyracea, the anterior skull base, or the middle turbinate and may also have multiple attachments to these structures. The pattern of attachment determines the position of the FSDP (Table 2, Fig. 7).
2. The uncinat process may be pneumatized (Fig. 8A) in 4% of the population or everted.<sup>8</sup>
3. An atelectatic uncinat process (Fig. 8B), commonly seen in maxillary sinus hypoplasia and silent sinus syndrome, is closely related to the inferior and medial wall of the ipsilateral orbit.<sup>11</sup> This increases the risk of inadvertent

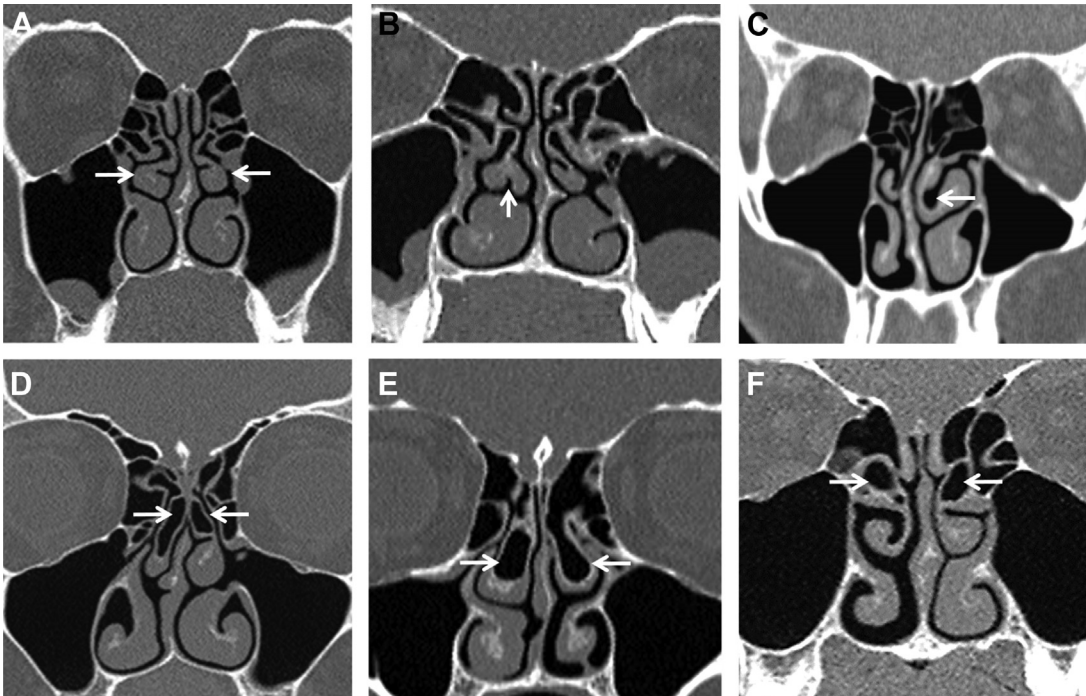


**Fig. 6.** Coronal CT images showing middle turbinate variants (arrows): (A) bilateral paradoxical turbinates, (B) bifid right middle turbinate, (C) left turbinate sinus, (D) bilateral interlamellar cells of Grunwald, (E) bilateral concha bullosa, and (F) bilateral pneumatized basal lamella.

**Table 2**  
Pattern of superior attachment of the uncinata process

Lamina Papyracea	Seen in more than 50% of individuals, <sup>12</sup> resulting in a medial FSDP draining into the middle meatus, creating a blind pouch laterally termed as the recessus terminalis
Anterior skull base	Results in a lateral FSDP opening into the ethmoidal infundibulum increasing chances of retrograde spread of infection into the frontal sinus from the ethmoidal sinus
Middle turbinate	FSDP is displaced posterior to the agger nasi cell, which needs to be fractured to access the FSDP <sup>11</sup>

From Vaid S, Vaid N. Normal Anatomy and Anatomic Variants of the Paranasal Sinuses on Computed Tomography. *Neuroimaging Clin N Am.* 2015 Nov;25(4):527 to 48.

orbital penetration during functional endoscopic sinus surgery (FESS).

- Rarely, the uncinata process may be absent<sup>17</sup> as seen in maxillary sinus hypoplasia.

### **The Frontal Sinus and Frontal Sinus Drainage Pathway**

The frontal sinuses develop as extensions from the anterior ethmoidal air cells. They may be absent in 5% and hypoplastic in 4% of the population.<sup>8</sup> Well-pneumatized frontal sinuses show typical scalloped margins with intact internal septa. The frontal beak (frontonasal process of the maxilla) forms an important surgical and imaging landmark in the anatomy of the FSDP.<sup>18</sup> It is identified on both coronal and parasagittal images (Fig. 9) with the frontal sinus superiorly and the FSDP inferiorly. The frontal beak corresponds to the level of the frontal ostium and hence its thickness determines the size of the frontal ostium. The agger nasi cell is the anterior-most extramural ethmoidal air cell, seen in 93% of the population,<sup>8</sup> and lies within the anterior portion of the FSDP. It is best viewed on parasagittal images and serves as an important surgical landmark.<sup>12</sup>

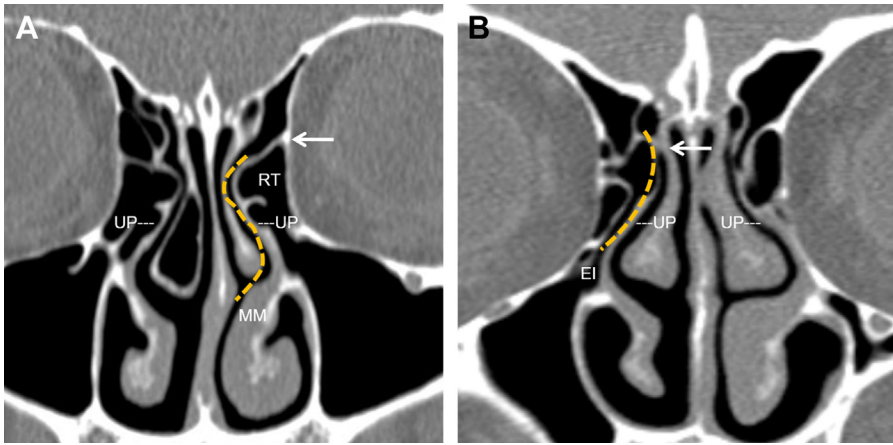


**Fig. 7.** Coronal CT images showing uncinete process attachments. (A) Left uncinete process (UP) attached to lamina papyracea (arrow) with the FSDP (dashed lines) draining into the medial meatus (MM), RT: recessus terminalis. (B) Right uncinete process attaching to the middle turbinate (arrow) with the FSDP (dashed lines) draining into the ethmoidal infundibulum (EI). (From Vaid S, Vaid N. Normal Anatomy and Anatomic Variants of the Paranasal Sinuses on Computed Tomography. *Neuroimaging Clin N Am.* 2015 Nov;25(4):527 to 48.)

### Anatomic Variants

1. Fronto-ethmoidal cells: The classification of frontal cells was first described by Kuhn in 1995<sup>8</sup> and modified by Wormald<sup>18</sup> (Table 3, Fig. 10). The authors also refer the readers to the latest classification of fronto-ethmoidal air cells (The International Frontal Sinus Anatomic Classification [2016] by Wormald<sup>19</sup>) used primarily by endoscopic sinus surgeons.
2. The frontal bullar cell arises superior to the bulla ethmoidalis and extends below the floor of the anterior cranial fossa, which forms the posterior border of this anatomic variant (Fig. 11).

### ANTERIOR ETHMOID SINUSES AND LAMELLAR ANATOMY

The anterior ethmoid sinuses are located anterior to the basal lamella. The largest cell in this group is the bulla ethmoidalis, which is a key surgical landmark during endoscopic sinus surgery. The cleft between the anterior margin of the bulla and the uncinete process is called the hiatus semilunaris.

#### Ethmoidal Lamellar Anatomy

Lamellae are organizational plates that develop within the cartilaginous olfactory capsule. They are important surgical landmarks and partition

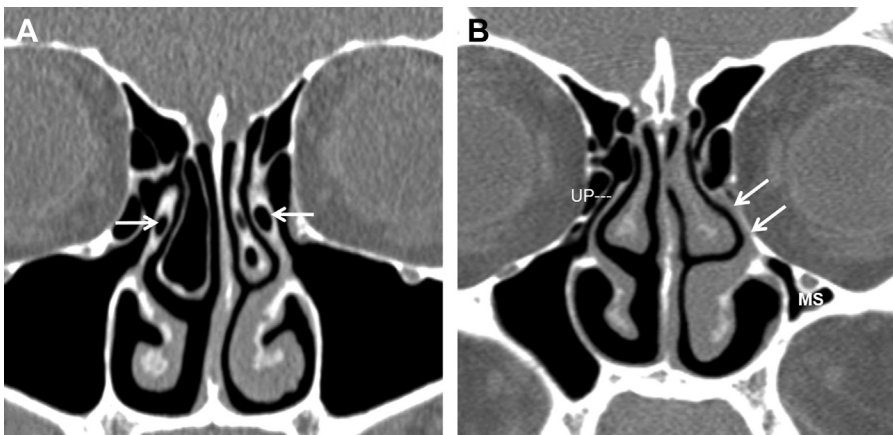


**Fig. 8.** Coronal CT images showing uncinete process variants (arrows): (A) bilateral pneumatized uncinete processes and (B) left atelectatic uncinete process owing to left maxillary sinus hypoplasia (MS). (From Vaid S, Vaid N. Normal Anatomy and Anatomic Variants of the Paranasal Sinuses on Computed Tomography. *Neuroimaging Clin N Am.* 2015 Nov;25(4):527 to 48.)

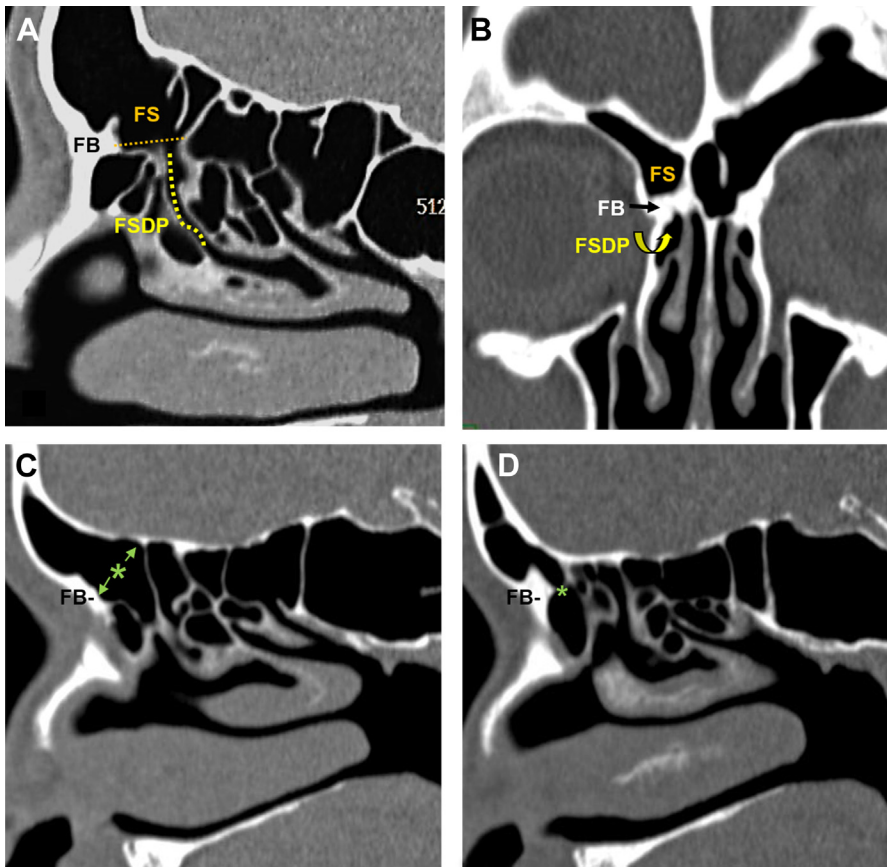


**Fig. 9.** Parasagittal (A) and coronal CT (B) showing frontal beak (FB) separating the frontal sinus (FS) above the dotted orange line in (A) from the FSDP (dotted yellow line in a, curved yellow arrow in b) below. Parasagittal CT sections (C–D) depict the impact of the frontal beak thickness (arrow) on the size of the frontal sinus ostium (green arrows/asterisk).

**Table 3**  
Classification of frontoethmoidal cells

Type 1 frontal cell	Single cell above the agger nasi and below the frontal beak (below the frontal ostium)
Type 2 frontal cells	Two or more cells above the agger nasi and below the frontal beak (below the frontal ostium)
Type 3 frontal cell	Single cell above the agger nasi with extension through the frontal ostium into the frontal sinus not exceeding 50% of the vertical height of the ipsilateral frontal sinus
Type 4 frontal cell	Single cell above the agger nasi with extension through the frontal ostium into the frontal sinus exceeding 50% of the vertical height of the ipsilateral frontal sinus, or an isolated cell within the frontal sinus
Frontal bullar cell	Single cell extending from the suprabullar region along the undersurface of the anterior skull base into the frontal sinus (anterior margin lies within the frontal sinus)
Interfrontal sinus septal cell	A cell associated with the frontal intersinus septum and may compromise the frontal ostium

From Vaid S, Vaid N. Normal Anatomy and Anatomic Variants of the Paranasal Sinuses on Computed Tomography. *Neuroimaging Clin N Am*. 2015 Nov;25(4):527 to 48.

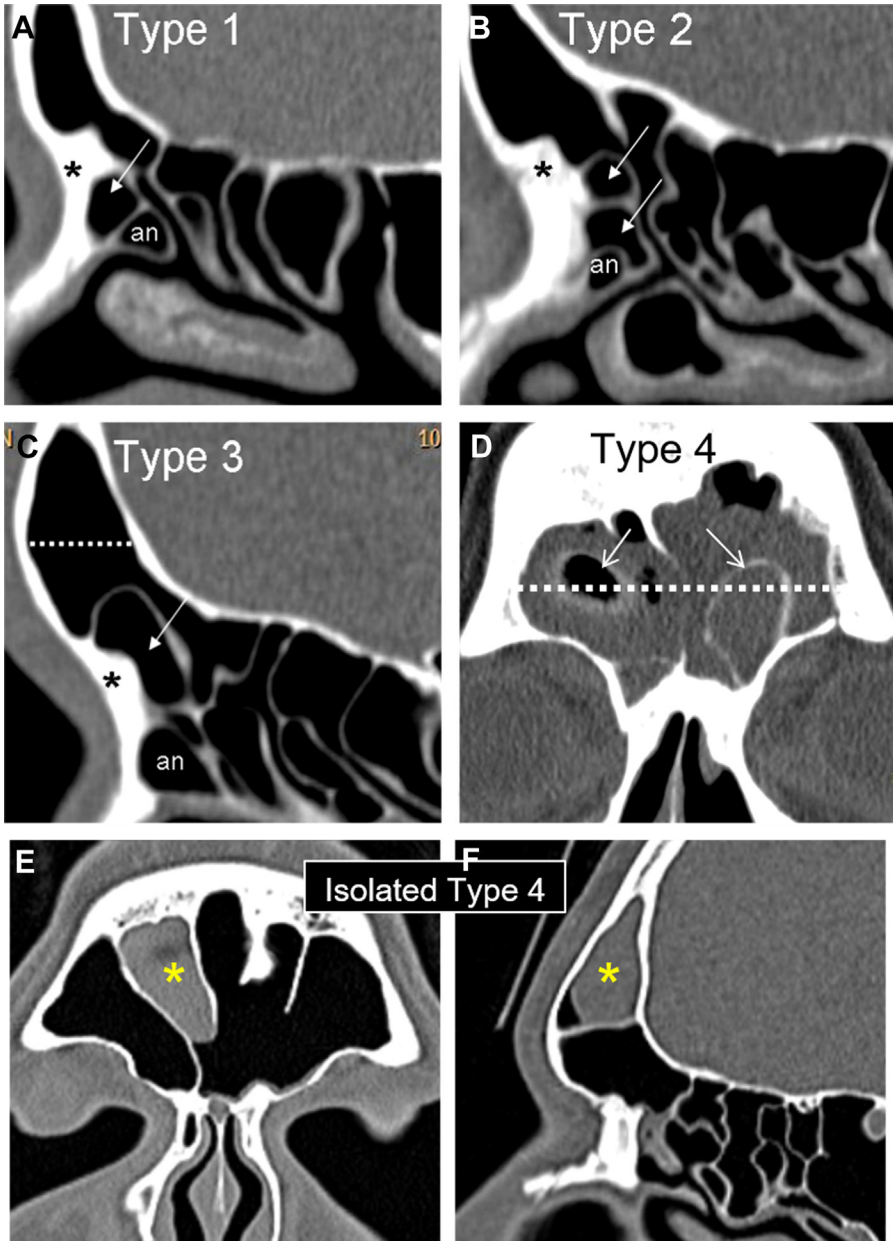


**Fig. 10.** Sagittal CT images (A–C) showing Types 1 to 3 fronto-ethmoidal cells (arrows). (D) Coronal CT image shows bilateral Type 4 fronto-ethmoidal cells (arrows). Frontal beak (asterisk); agger nasi (an). The dotted white line depicts the midpoint of the height of the ipsilateral frontal sinus. Coronal (D & E) and sagittal (F) images depict opacified and superiorly located Type 4 fronto-ethmoidal cell.

the sinonasal cavity into well-defined compartments.<sup>12</sup> The lamellae course through the ethmoidal air cells and extend superiorly up to the skull base from the lateral nasal wall. These structures are best seen in the parasagittal planes (Fig. 12) and from anterior to posterior include the uncinete process, anterior margin of the bulla ethmoidalis, lamella of the middle turbinate (basal lamella), lamella of the superior turbinate, and, if

present, the lamella of the supreme turbinate. If the supreme turbinate is absent, the anterior face of the sphenoid sinus is considered the fifth lamella.

#### Anatomic Variants

1. The suprabullar recess lies between the superior wall of the bulla ethmoidalis and the roof

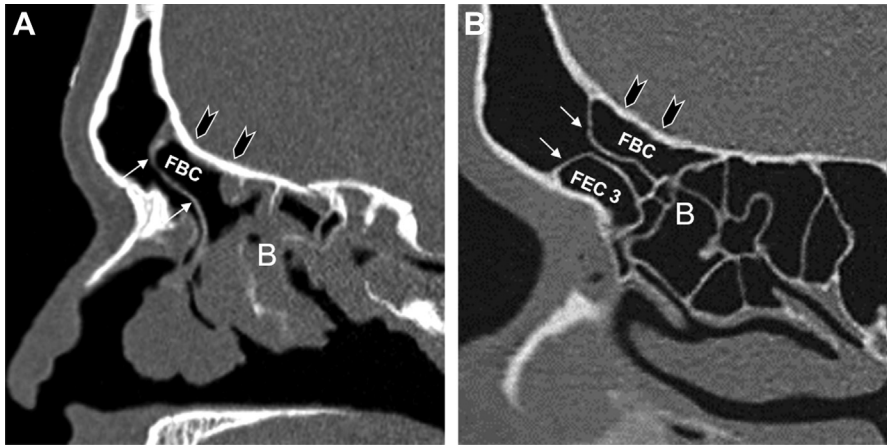


**Fig. 11.** Parasagittal image (A) shows a large frontal bullar cell (FBC), above the bulla ethmoidalis (B) with anterior margin related to the frontal sinus (arrows) and posterior margin formed by the anterior skull base (arrowheads). Arrows in parasagittal image (B) show the difference between the superiorly located FBC and the inferiorly located Type 3 fronto-ethmoidal cell (FEC 3).

of the ethmoid sinus and is best appreciated on a parasagittal image (Fig. 13A). This recess can extend laterally as supraorbital cells (Fig. 13B).

- Anterior ethmoidal air cells extending along the floor of the orbits, lateral to the sagittal plane of the lamina papyracea are called Haller cells (Fig. 14A), reported in 10% to 45% of the patients.<sup>8</sup> The inferomedial strut line of the orbit is a useful anatomic structure to differentiate between bulla ethmoidalis cell (above the line) and Haller cells (below the line; Fig. 14B, C).<sup>20</sup> Haller cells narrow the maxillary sinus ostium.

### The Maxillary Sinus and Ostiomeatal Complex

The maxillary sinus or antrum occupies the body of the maxillary bone. The roof is formed by the orbital floor, and the floor is formed by the alveolar process of the maxilla. The infraorbital nerve (a branch of the maxillary division of the trigeminal nerve) runs in a bony canal along the roof of the maxillary sinus. The maxillary ostium is located along the superior aspect of the medial wall of the sinus and drains into the base of the ethmoidal infundibulum.<sup>12</sup> The components of the ostiomeatal complex or unit as identified on coronal CT (Fig. 15) comprise the maxillary ostium, the middle

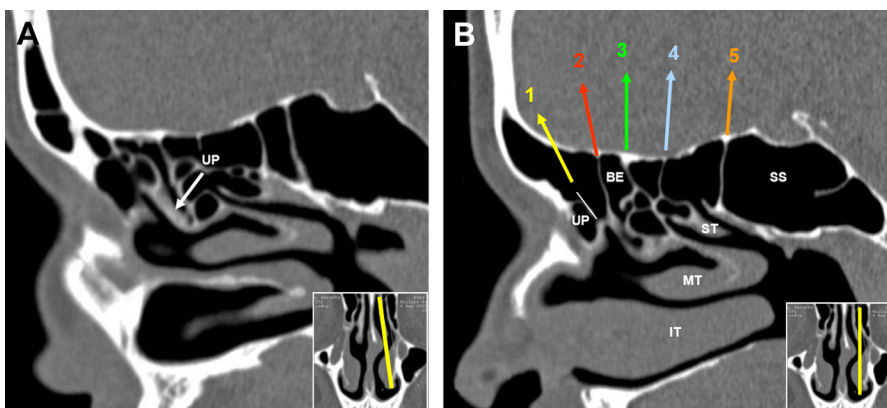


**Fig. 12.** Sagittal oblique (A) and sagittal (B) CT images showing lamellar anatomy: 1: uncinete process (UP: white arrow in a). 2: anterior margin of bulla ethmoidalis (BE). 3: basal lamella MT: middle turbinate. 4: lamella of the superior turbinate (ST). 5: anterior margin of the sphenoid sinus (SS). IT: inferior turbinate. (From Vaid S, Vaid N. Normal Anatomy and Anatomic Variants of the Paranasal Sinuses on Computed Tomography. *Neuroimaging Clin N Am.* 2015 Nov;25(4):527 to 48.)

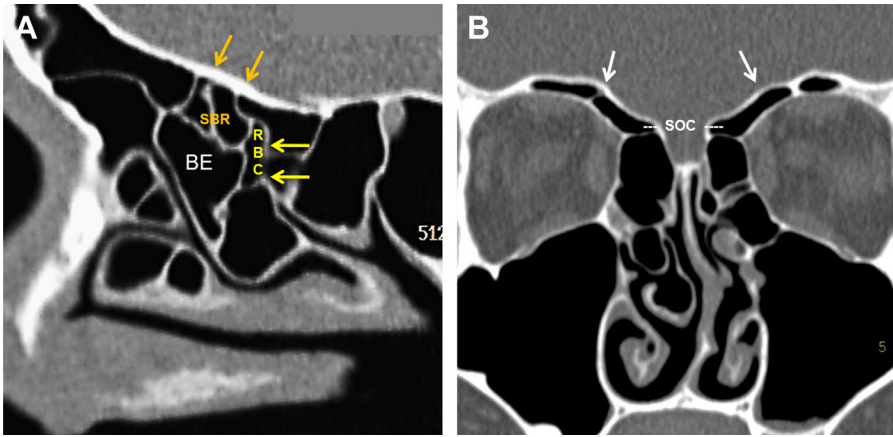


**Fig. 13.** Sagittal CT image (A) shows the suprabullar recess (SBR) and the retro-bullar cleft (RBC). Coronal CT image (B) shows bilateral supraorbital cells (arrows).

meatus, the ethmoidal infundibulum, the bulla ethmoidalis, the uncinata process, and the hiatus semilunaris.<sup>12</sup>

### Anatomic Variants

1. Reduced size of the maxillary sinus is seen in hypoplasia (in up to 10% of the population), silent sinus syndrome and following trauma/surgery (Fig. 16). The congenitally small maxillary sinus is associated with posterior and inferior displacement of the globe. The lamina papyracea in such cases is also lateralized with an increase in the retro-antral fat and thickening of the bony walls (increase in the height of the alveolar process).<sup>21</sup>
2. In hyperpneumatized maxillary sinuses, there is a thin mucosal lining between the maxillary antrum and the dental roots, which can protrude into the sinus. This can predispose to recurrent sinusitis from dental infections and to oroantral fistulas following dental extraction.<sup>22</sup>
3. Septa within the maxillary sinuses are common and may be fibrous or bony. They usually extend from the infraorbital nerve canal to the lateral wall and can affect the drainage of the maxillary sinuses.<sup>12</sup> Bony margins of the infraorbital nerve canal may be dehiscent in up to 14% of cases.<sup>8</sup>
4. Accessory ostia are seen in 10% to 25% of the population, located within the region of the posterior fontanelle, behind the natural ostia.<sup>8</sup> The posterior fontanelle is a bony defect in the lateral nasal wall (medial wall of the maxillary sinus) located superior to the insertion of the inferior turbinate.

### The Lamina Papyracea and Anterior Ethmoidal Artery

The lamina papyracea form the lateral walls of the ethmoid sinuses separating them from the adjacent orbits. Focal corticated defects in the lamina papyracea are seen in up to 0.5% to 10% of the population and are not clinically significant.<sup>12</sup>

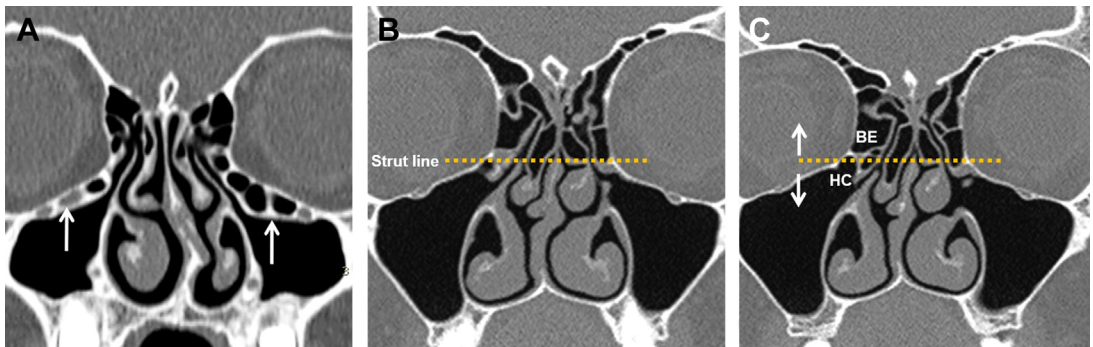


**Fig. 14.** Haller cells (arrows in A). The inferomedial strut line of the orbit (dotted orange line in B and C) is a useful anatomic structure to differentiate between the bulla ethmoidalis (BE) and Haller cells (HC).

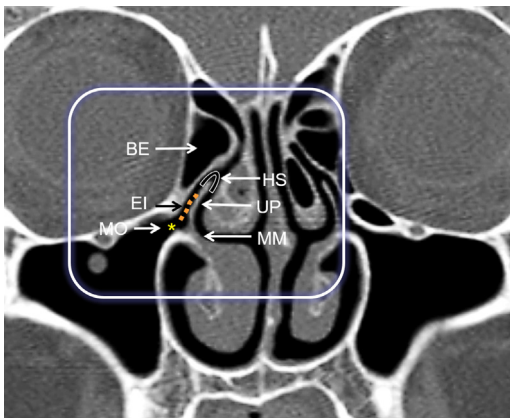


**Fig. 15.** Coronal CT image showing components of the OMC. MO: maxillary ostium (*asterisk*); EI: ethmoidal infundibulum (*dotted line*); BE: bulla ethmoidalis; MM: middle meatus; UP: uncinate process; HS: hiatus semilunaris (*curved block*).

Larger defects (congenital, posttraumatic, or postoperative) in the lamina (**Fig. 17**) need preoperative documentation to avoid inadvertent orbital injury. Defects in the posterior lamina papyracea are more significant because there is a relatively thinner fat pad between the medial rectus muscle and the lamina papyracea with increased chances of orbital injury.<sup>23</sup>

The ethmoidal segment of the AEA (branch of the ophthalmic artery) enters the ethmoid sinus through the olfactory floor and passes superiorly into the anterior skull base. Cadaveric and live dissection studies have shown that the AEA is most often located between the second (anterior margin of the bulla ethmoidalis) and the third lamella (lamella of the middle turbinate; basal lamella).<sup>24</sup> It courses in a bony canal (anterior ethmoidal canal [AEC]) through the upper one-third of the lamina papyracea. This canal can be

best identified on coronal CT by a beak-like projection of the medial orbital wall behind the bulla ethmoidalis. Two parallel hyperdense lines extending into the adjacent ethmoid sinus mark the precise location of the AEA (**Fig. 18A**).<sup>8</sup> The AEC together with the AEA is also well visualized on parasagittal images (**Fig. 18C–E**) and can be graded based on the location with respect to the skull base.<sup>25</sup>

- Grade I AEC: located within the ethmoidal roof.
- Grade II AEC: located under the roof.
- Grade III AEC: located distant from the ethmoidal roof.

### Anatomic Variant

Normal bony covering of the anterior ethmoidal artery may be absent and the canal may be dehiscent inferiorly into the anterior ethmoidal air cells in up to 66% of cases.<sup>24,25</sup> In these cases, the artery is suspended on a mucous membrane mesentery below the skull base, and is prone to injury during surgery, especially if the bony canal is deficient (**Fig. 18B, F**).

### The Anterior Skull Base: Olfactory Fossa and Height of the Ethmoid Skull Base

#### The olfactory fossa

The olfactory fossa, containing the olfactory bulbs, is formed by the crista galli medially, medial lamella of the cribriform plate inferiorly, and lateral lamella of the cribriform plate laterally. Three types of olfactory fossae were described by Keros<sup>26</sup> based on the length of the lateral lamella of the cribriform plate (**Table 4, Fig. 19A–C**). The lateral lamella of the cribriform plate is structurally the thinnest bone in the anterior skull base and dehiscent in up to 14% of patients.<sup>8</sup>

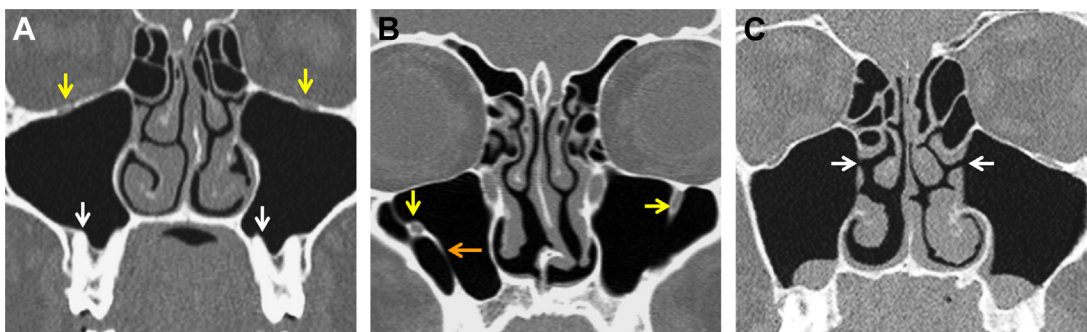


**Fig. 16.** Coronal CT images showing maxillary sinus variants (*arrows*): (A) maxillary dental roots protruding into the sinus floor, normal infraorbital nerve canals (*yellow arrows*). (B) bilateral dehiscent infraorbital nerve canals (*yellow arrows*) with an intrasinus septum (*orange arrow*) attaching to the dehiscent canal on the right side. (C) bilateral accessory ostia.

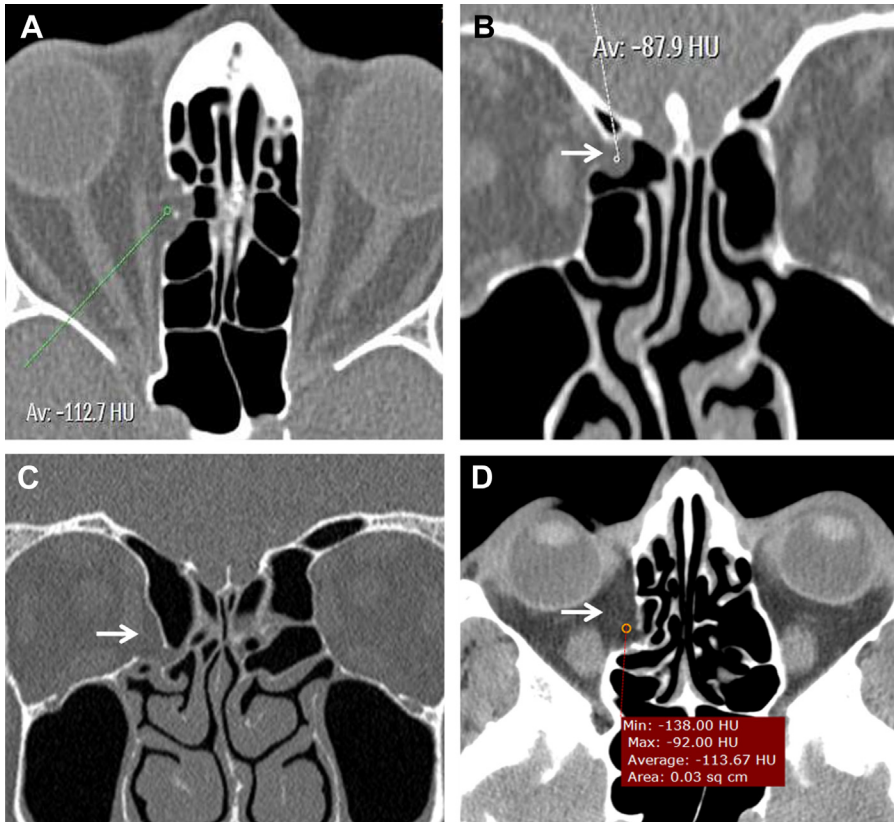


**Fig. 17.** Axial (A, D) and coronal (B, C) CT images showing focal dehiscence of the right lamina papyracea (arrow). Intraorbital fat herniates through the defect into the ethmoid sinuses.

### Anatomic Variant

Asymmetry in the level of the olfactory fossa occurs in up to 10% to 30% of the population (Fig. 19D). The angle between the medial and lateral lamella of the cribriform plate is also variable.<sup>12</sup> Bates and Massoud<sup>27</sup> propose changes in the nomenclature surrounding the term “olfactory” for improved uniformity and accuracy. Fig. 20 depicts the olfactory groove, olfactory recess, olfactory vestibule, and the olfactory cleft as proposed by these authors.

### Height of the Ethmoid Skull Base

The roof of the anterior ethmoid sinus is formed by the fovea ethmoidalis laterally and the cribriform plate medially. The height of the ethmoid skull base (ESB) can be assessed by 2 methods proposed by Myers and Valvasorri<sup>28</sup> and more recently by Rudmik and Smith<sup>29</sup> (Table 5, Fig. 21).

### Anatomic Variant

A low ESB indicates a dangerously low lying and medially sloping anterior skull base with higher

chances of intraoperative intracranial penetration.<sup>29</sup>

### The Posterior Sinus Group: Posterior Ethmoid Sinus and Sphenoid Sinus

#### The posterior ethmoid sinus

The posterior ethmoidal air cells are located between the basal lamella and the sphenoid sinus and are fewer in number than the anterior ethmoidal cells. The lamina papyracea lies laterally and the superior turbinate forms the medial boundary of this sinus group that drains into the superior meatus.

### Anatomic Variant

Spheno-ethmoidal cell (Onodi cell): As the posterior ethmoidal cells pneumatize before the sphenoid sinus, they have a high propensity to grow above and lateral to the developing sphenoid sinus forming the Onodi cell. This is seen in 3.4% to 14% of the general population.<sup>8</sup> An Onodi cell should be suspected on coronal CT images that show an obliquely oriented or horizontal septum within the sphenoid sinus (Fig. 22A & B). Some

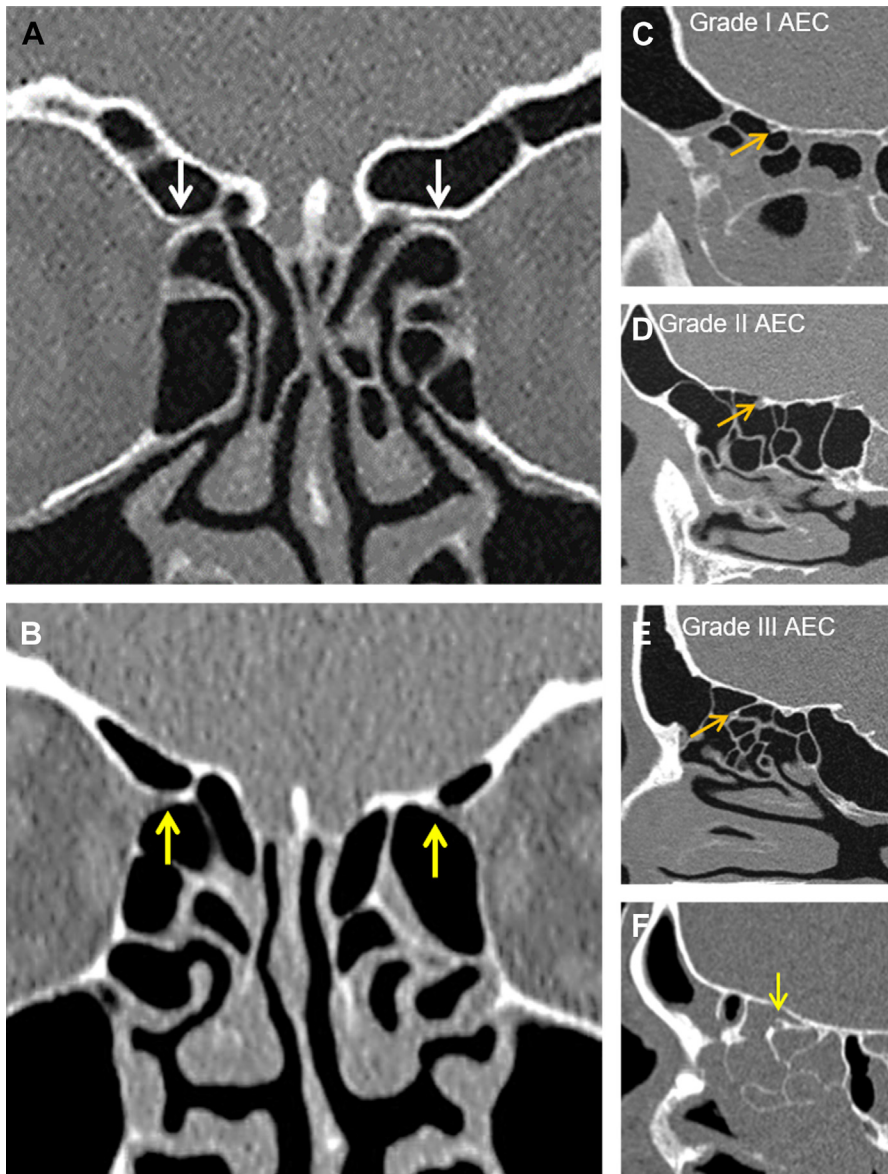


**Fig. 18.** Coronal CT images showing (A) normal bony canal for the anterior ethmoidal arteries (vertical white arrows) and (B) both arteries suspended in a mesentery without bone cover (vertical yellow arrows). Parasagittal images (C–E) depict grades of the AEC with respect to the skull base (oblique orange arrows). Short vertical yellow arrow in (F) depicts a focal defect in the bony canal for the AEA.

**Table 4**  
Keros classification of the olfactory fossa

Type 1	Length of the lateral lamella is 1–3 mm indicating a shallow or flat olfactory fossa seen in 30% of cases
Type 2	Length of the lateral lamella is 4–7 mm indicating a moderately deep olfactory fossa seen in 49% of cases
Type 3	The lateral lamella is longer measuring 8–16 mm with a resultant deep olfactory fossa seen in 21% of cases <sup>16</sup>

From Vaid S, Vaid N. Normal Anatomy and Anatomic Variants of the Paranasal Sinuses on Computed Tomography. *Neuroimaging Clin N Am.* 2015 Nov;25(4):527 to 48.

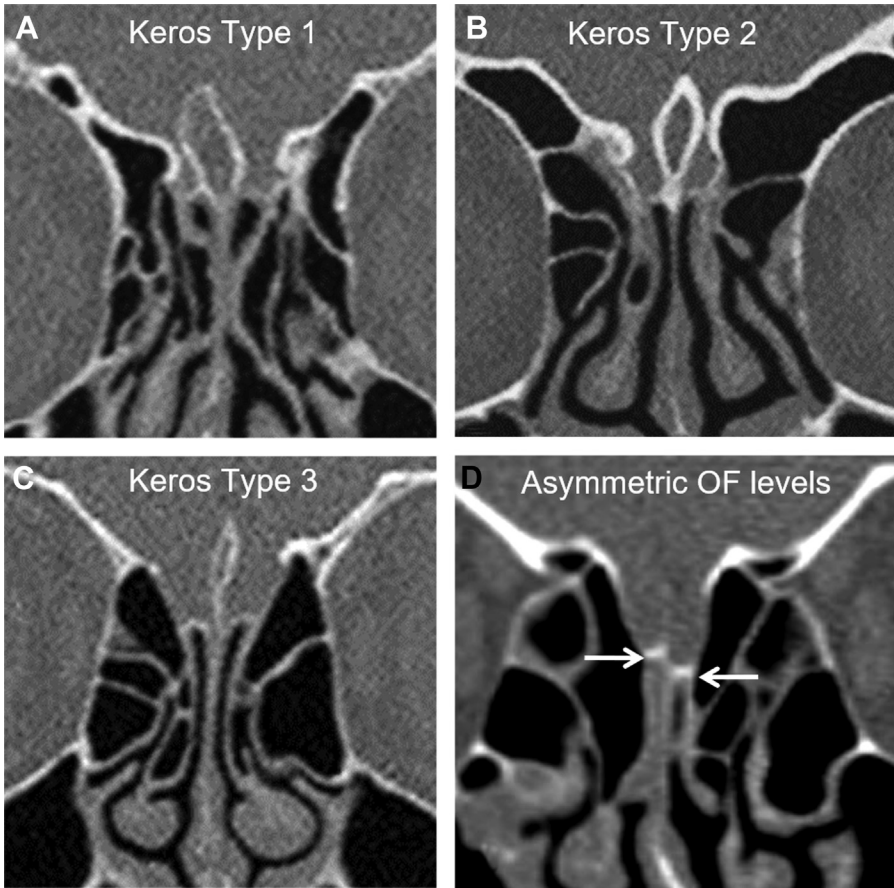


**Fig. 19.** Coronal CT images depicting Keros classification of olfactory fossae (A–C). Asymmetrical levels of the olfactory fossae (arrows in D).

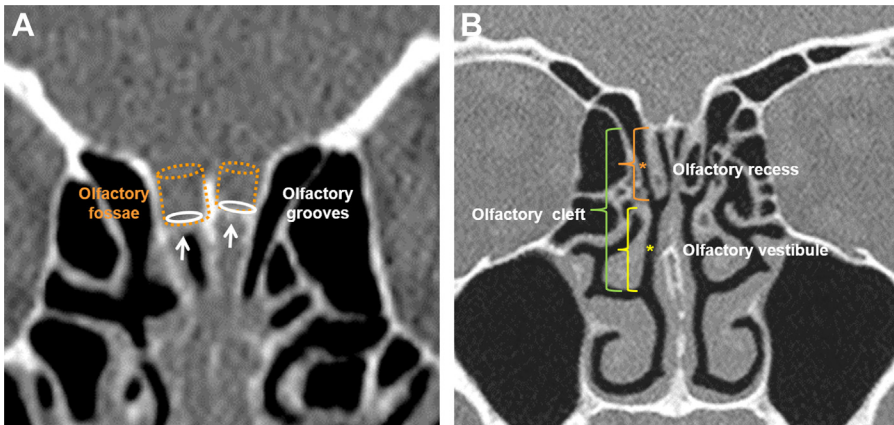


**Fig. 20.** Coronal CT image depicts the location and extent of the olfactory fossae and groove (A). The olfactory recess (medial lamella of the cribriform plate down to the basal lamella of the middle turbinate), the olfactory vestibule (basal lamella down to the lower margin of the middle turbinate), and the olfactory cleft (olfactory recess and vestibule together) are depicted in (B).

**Table 5**  
**Estimation of the height of the ethmoidal skull base**

Authors	Methodology	Interpretation
Myers and Valvasorri <sup>28</sup> 1998	The vertical height of the orbit is divided into 3 equal sections. The position of the ESB is documented in reference to upper, middle, or lower one-third of the vertical orbital height	If the ESB passes above the upper one-third of the vertical height of the ipsilateral orbit it indicates a normal and hence a surgically safe ESB. An ESB passing through or below the midorbital plane is considered a low ESB
Rudmik and Smith <sup>29</sup> 2012	The vertical distance between the height of the ESB and the midorbital plane is measured in a coronal CT image showing the canal for the anterior ethmoidal artery	In their study, the mean height of the ESB was found to be 8.5 mms. A vertical height of more than 8.5 mms was considered a safe and high ESB, a measurement between 4 and 7 mms was considered as a moderately safe ESB and a height less than 4 mms was deemed as a low and surgically unsafe ESB with high chances of inadvertent intracranial penetration

From Vaid S, Vaid N. Normal Anatomy and Anatomic Variants of the Paranasal Sinuses on Computed Tomography. *Neuroimaging Clin N Am.* 2015 Nov;25(4):527 to 48.

authors have proposed a “cruciform sign” to diagnose bilateral Onodi cells (Fig. 22C), in which a coronal CT image at the level of the posterior choana demonstrates the sphenoid air cell showing cruciform septation.<sup>11</sup> Important critical relationships of the sphenoid sinus, namely the optic nerves and internal carotid arteries are directly related to the posterior ethmoid sinuses in the presence of Onodi cells.

### The Sphenoid Sinus

The sphenoid sinus develops in the body of the sphenoid bone and is generally bilateral although asymmetric in size.<sup>8</sup> The sphenoid sinus is classified into 4 types depending on the degree of pneumatization<sup>30</sup> (Table 6, Fig. 23). Several bony canals and foramina transmit critical neurovascular structures related to the sphenoid sinus (Table 7). The anterior clinoid processes may be

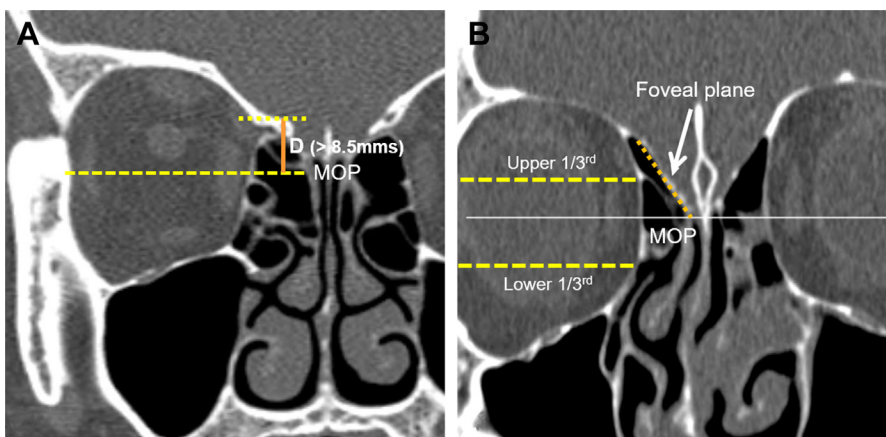


**Fig. 21.** ESB height. Coronal CT image (A) showing ESB height with normal vertical distance (D) between the mid-orbital plane (MOP, dashed line) and the anterior skull base (dotted line) (see Table 5). Coronal CT image (B) showing a low-lying foveal plane (dotted orange line/arrow) reaching the mid-orbital plane (horizontal white line). The dashed yellow lines depict the division of the vertical height of the orbit as reference planes (see Table 5). (From Vaid S, Vaid N. Normal Anatomy and Anatomic Variants of the Paranasal Sinuses on Computed Tomography. *Neuroimaging Clin N Am.* 2015 Nov;25(4):527 to 48.)

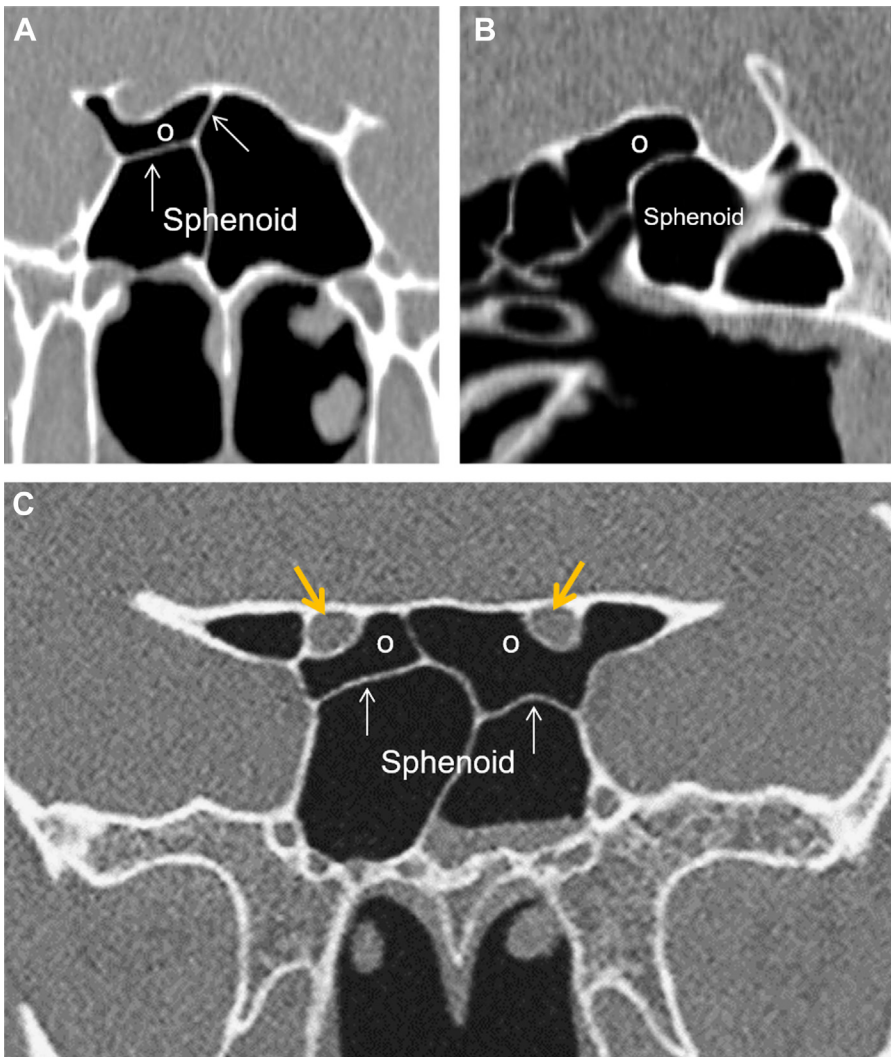


**Fig. 22.** Coronal (A) and sagittal (B) CT images showing a right Onodi cell (O) with obliquely oriented intrasinus septa (arrows). Coronal image (C) shows the “cruciform sign” seen with bilateral Onodi cells (O). Both optic nerves course through these cells (arrows).

**Table 6**  
**Classification of type of sphenoid sinus**

Sphenoid sinus Agenesis	A nonpneumatized sphenoid sinus seen in <0.7% of individuals
Conchal sphenoid sinus	A small rudimentary air cavity within the sphenoid bone not reaching up to the anterior wall of the sella tursica seen in 1%–4% of the population
Presellar sphenoid sinus	The posterior sinus wall extends up to the anterior wall of the sella tursica seen in 35%–40% of the population
Sellar sphenoid sinus	The sinus cavity extends beyond the anterior wall of the sella tursica below the pituitary fossa seen in 55%–60% of the population. Wang J and others <sup>30</sup> further classified this type of sphenoid sinus more recently based on the direction of pneumatization into sphenoid body, lateral clivus, lesser sphenoid wing, anterior rostral, and the combined variety

From Vaid S, Vaid N. Normal Anatomy and Anatomic Variants of the Paranasal Sinuses on Computed Tomography. *Neuroimaging Clin N Am.* 2015 Nov;25(4):527 to 48.

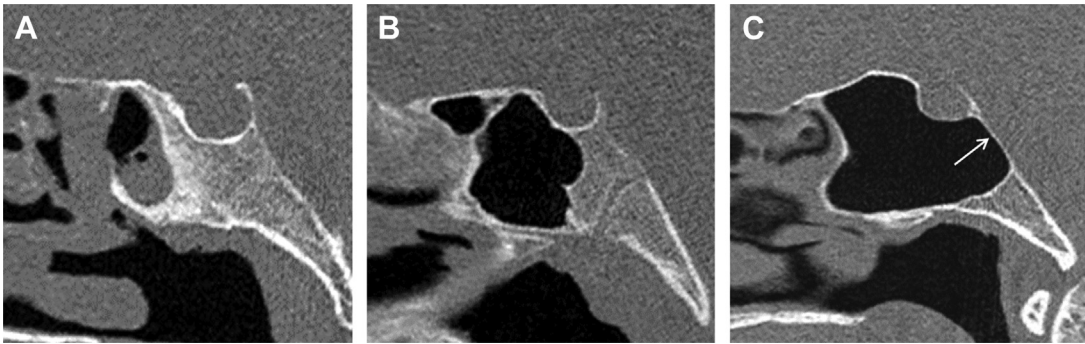


**Fig. 23.** Sagittal CT images show (A) conchal, (B) presellar, and (C) sellar variants of sphenoid sinus pneumatization. The sellar variant may have a thin posterior bony margin (arrow) with a potential risk of intraoperative skull base trauma.

pneumatized in up to 6% to 13% of cases<sup>8</sup> forming the carotico-optic recess between the optic nerve above and the internal carotid artery below.

### Anatomic Variants

1. Intrasinus septa attached to the bony walls of the internal carotid artery and optic nerve need preoperative identification because excessive traction on these septa may lead to an avulsion of the bony walls and catastrophic complications (Fig. 24).
2. The position of the neurovascular structures around the sphenoid sinus is determined by

the degree of pneumatization. Occasionally, the structures are exposed within the sinus cavity and connected to the sinus walls by bony stalks.

3. Persistence of the lateral craniopharyngeal canal in association with sphenoid hyperpneumatization and raised intracranial pressure may lead to the formation of a spontaneous lateral sphenoid meningoencephalocele and spontaneous cerebrospinal fluid leak.
4. In approximately 80% of cases of anterior clinoid process pneumatization, the optic nerve will be dehiscient into the superolateral aspect of the sphenoid sinus.<sup>31</sup>

**Table 7**

#### Critical neurovascular/congenital channels related to the sphenoid sinus

Optic nerve canals	Related to the roof of the sphenoid sinus. Bony walls can be dehiscient in up to 24% of cases. <sup>8</sup> Delano et al classified the optic nerves into 4 categories based on the relationship of the nerve with the sphenoid and posterior ethmoid sinuses (31)
The internal carotid artery canals	Located along the posterolateral wall of the sphenoid sinus and the bony coverings may be dehiscient in up to 25% of cases <sup>3</sup>
The pterygoid canals (vidian canals)	Along the inferior sinus walls that transmit the combined great petrosal and deep petrosal nerve complex as well as the artery and vein of the pterygoid canal
Foramen rotundum	Along the lateral sinus walls which transmit the maxillary division of the trigeminal nerve, artery of the foramen rotundum, and an emissary vein
Lateral craniopharyngeal canal (Sternberg's canal)	Represents a congenital bony defect in the lateral wall of the sphenoid sinus situated further lateral to the maxillary nerve

From Vaid S, Vaid N. Normal Anatomy and Anatomic Variants of the Paranasal Sinuses on Computed Tomography. *Neuroimaging Clin N Am.* 2015 Nov;25(4):527-48.

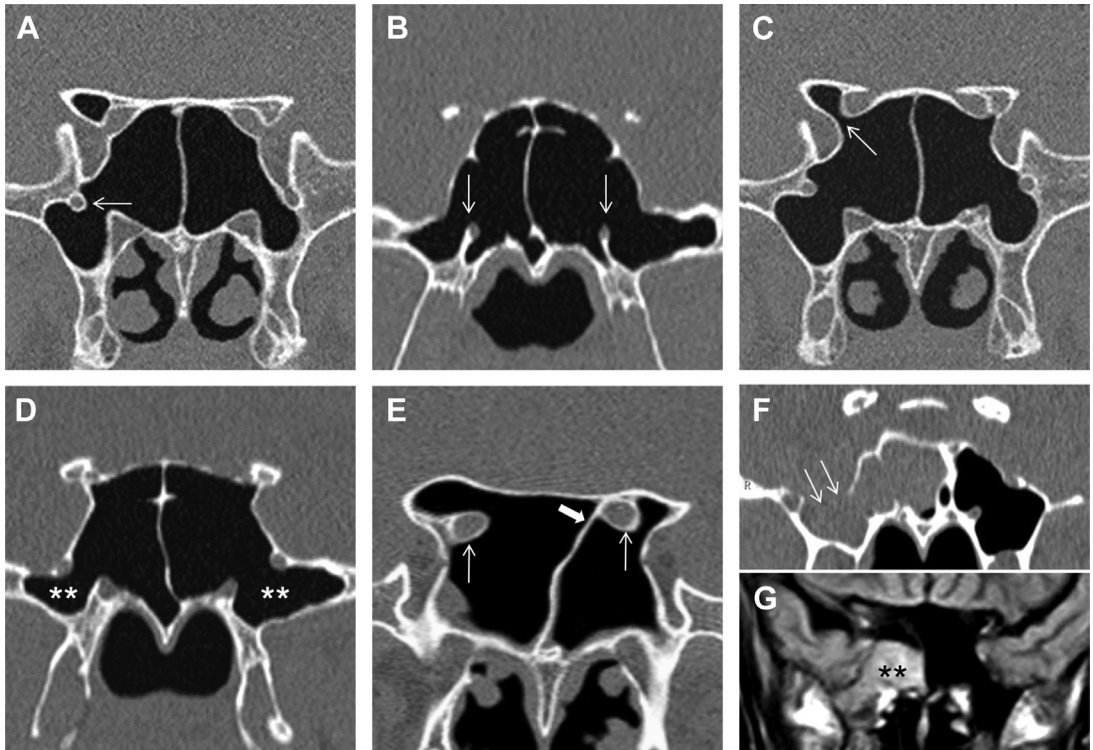


**Fig. 24.** Coronal CT images showing sphenoid sinus variants (*arrows*). (A) Endosinal right foramen rotundum and endosinal vidian canals (B). Right carotico-optic recess (C) and prominent lateral recesses (\*\* in D). Bilateral optic nerve dehiscence (E) with intrasinus septum attaching to left optic nerve canal (block arrow). Widened lateral craniopharyngeal canal on the right side (F) with coronal T1W MR image (G) showing an associated meningoencephalocele (\*\*).

## SUMMARY

A structured approach to CT scans of the PNSs using multiplanar imaging enables a better understanding of the complex anatomy of this region and its numerous anatomic variants. Radiologists need to be aware of the critical clinical implications of identifying these anatomic variations.

## CLINICS CARE POINT 1

Multiplanar CT evaluation of PNSs in orthogonal and nonorthogonal planes is important to outline the anatomy and identify surgically important anatomic variants.

Pre-FESS CT examinations of the PNSs are usually noncontrast-enhanced studies. Contrast examinations are reserved for evaluating specific pathologic conditions (aggressive infections, neoplasm, and vascular lesions) and for assessing extension into orbit, intracranial compartment, and surrounding soft tissues.

Knowledge of relevant embryologic events in paranasal sinus development can avoid pitfalls

in diagnosis. Sinus pathologic conditions in children aged younger than 4 years are uncommon except in the ethmoid sinuses because these are the only sinuses, which are pneumatized at birth.

## CLINICS CARE POINT 2

Important nerves and vessels related to the PNSs include the following:

- Infraorbital nerves along the roof of the maxillary sinus.
- Optic nerves.
- Internal carotid arteries.
- Pterygoid artery and vein and the great petrosal-deep petrosal nerve complex in the vidian canal.
- Maxillary division of the trigeminal nerve in the foramen rotundum.

### CLINICS CARE POINT 3

The use of the mnemonic "CLOSE" enables the radiologist to identify and report important and surgically relevant sinonasal anatomical variants.<sup>32</sup>

C: Cribriform plate anatomy.

L: Lamina papyracea integrity.

O: Optic nerve anatomy

S: Sphenoid sinus anatomy, internal carotid artery (ICA) anatomy, and presence of the Onodi cell

E: Ethmoidal (anterior) artery anatomy

### DISCLOSURE

The authors state that there are no commercial or financial conflicts of interest and no funding sources to declare.

### SUPPLEMENTARY DATA

Supplementary data related to this article can be found online at <https://doi.org/10.1016/j.nic.2022.07.007>.

### REFERENCES

- Ónodi A, Thomson SC. The anatomy of the nasal cavity and its accessory sinuses: an atlas for practitioners and students. London: H.K. Lewis; 1895.
- Aksoy EA, Özden SU, Karaarslan E, et al. Reliability of high-pitch ultra-low-dose paranasal sinus computed tomography for evaluating paranasal sinus anatomy and sinus disease. *J Craniofac Surg* 2014;25(5):1801–4.
- Dahmani-Causse M, Marx M, Deguine O, et al. Morphologic examination of the temporal bone by cone-beam computed tomography: comparison with multislice helical computed tomography. *Eur Ann Otorhinolaryngol Head Neck Dis* 2011;128:230–5.
- Bremke M, Leppek R, Werner JA. Digital volume tomography in ENT medicine. *HNO* 2010;58(8):823–32.
- Wormald PJ. Imaging in Endoscopic Sinus Surgery. In: Wormald PJ, editor. *Endoscopic sinus surgery: anatomy, three-dimensional reconstruction, and surgical technique*. 3rd edition. New York, NY: Thieme Medical Publishers; 2013. p. 13–8.
- Marquez S, Tessema B, Clement PA, et al. Development of the ethmoid sinus and extramural migration: the anatomical basis of this paranasal sinus. *Anat Rec (Hoboken)* 2008;291(11):1535–53.
- Goldman-Yassen AE, Meda K, Kadom N. Paranasal sinus development and implications for imaging. *Pediatr Radiol* 2021;51(7):1134–48.
- Vaid S, Vaid N. Normal Anatomy and Anatomic Variants of the Paranasal Sinuses on Computed Tomography. *Neuroimaging Clin N Am* 2015;25(4):527–48.
- Shafik AG, Rabie TM, Alkady HA, et al. Evaluation of the Internal Nasal Valve using Computed Tomography Pre and Post Rhinoplasty and Its Correlation to Symptomatic Improvement. *Egypt J Hosp Med* 2018;72(5):4486–9.
- Moche JA, Cohen JC, Pearlman SJ. Axial computed tomography evaluation of the internal nasal valve correlates with clinical valve narrowing and patient complaint. *Int Forum Allergy Rhinol* 2012;3(7):592–7.
- Beale TJ, Madani G, Morley SJ. Imaging of the paranasal sinuses and nasal cavity: normal anatomy and clinically relevant anatomical variants. *Semin Ultrasound CT MR* 2009;30(1):2–16.
- Vaid S, Vaid N, Rawat S, et al. An imaging checklist for pre-FESS CT: framing a surgically relevant report. *Clin Radiol* 2011;66(5):459–70.
- Bolger WE, Butzin CA, Parsons DS. Paranasal sinus bony anatomic variations and mucosal abnormalities: CT analysis for endoscopic sinus surgery. *Laryngoscope* 1991;101:56–64.
- Calvo-Henríquez C, Ruano-Ravina A, Martínez-Capoccioni G, et al. The lamellar cell: a radiological study and a new classification proposal. *Eur Arch Otorhinolaryngol* 2018;275(11):2713–7.
- Cellina M, Gibelli D, Cappella A, et al. Nasal cavities and the nasal septum: Anatomical variants and assessment of features with computed tomography. *Neuroradiol J* 2020;33(4):340–7.
- Lund VJ, Stammberger H, Fokkens WJ, et al. European position paper on the anatomical terminology of the internal nose and paranasal sinuses. *Rhinol Suppl* 2014;24:1–34.
- Bolger WE, Woodruff WW, Morehead J, et al. Maxillary sinus hypoplasia: classification and description of associated uncinat process hypoplasia. *Otolaryngol Head Neck Surg* 1990;103(5):759–65.
- Wormald PJ. Anatomy of the frontal recess and frontal sinus with three-dimensional reconstruction. In: Wormald PJ, editor. *Endoscopic sinus surgery: anatomy, three-dimensional reconstruction, and surgical technique*. 4th edition. New York: Thieme Medical Publishers; 2018. p. 52–88.
- Wormald PJ, Hoseman W, Callejas C, et al. The International Frontal Sinus Anatomy Classification (IFAC) and Classification of the Extent of Endoscopic Frontal Sinus Surgery (EFSS). *Int Forum Allergy Rhinol* 2016;6(7):677–96.
- Kim JW, Goldberg Robert A, Shorr N. The Inferomedial Orbital Strut An Anatomic and Radiographic Study. *Ophthalmic Plast Reconstr Surg* 2002;18(5):355–64.

21. Whyte A, Boeddinghaus R. The maxillary sinus: physiology, development and imaging anatomy. *Dentomaxillofac Radiol* 2019;48(8):20190205. Erratum in: *Dentomaxillofac Radiol*. 2019;10.1259:20190205c.
22. Whyte A, Boeddinghaus R. Imaging of odontogenic sinusitis. *Clin Radiol* 2019;74(7):503–16.
23. Bhatti MT, Schmalfuss IM, Mancuso AA. Orbital complications of functional endoscopic sinus surgery: MR and CT findings. *Clin Radiol* 2005;60:894–904.
24. Guarnizo A, Nguyen TB, Glikstein R, et al. Computed tomography assessment of anterior ethmoidal canal dehiscence: An interobserver agreement study and review of the literature. *Neuroradiol J* 2020;33(2):145–51.
25. Lannoy-Penisson L, Schultz P, Riehm S, et al. The anterior ethmoidal artery: radio anatomical comparison and its application in endonasal surgery. *Acta Otolaryngol* 2007;127:618–22.
26. Keros P. On the practical value of differences in the level of the lamina cribrosa of the ethmoid. *Z Laryngol Rhinol Otol* 1962;41:809–13.
27. Bates NS, Massoud TF. Ambiguous “olfactory” terms for anatomic spaces adjacent to the cribriform plate: A publication database analysis and quest for uniformity. *Clin Anat* 2021;34(8):1186–95.
28. Meyers RM, Valvassori G. Interpretation of anatomic variations of computed tomography scans of the sinuses: a surgeon’s perspective. *Laryngoscope* 1998;108:422–5.
29. Rudmik L, Smith TL. Evaluation of the Ethmoid Skull Base Height Prior to Endoscopic Sinus Surgery: A Preoperative CT Evaluation Technique. *Int Forum Allergy Rhinol* 2012;2(2):151–4.
30. Wang J, Bidari S, Inoue K, et al. Extensions of the sphenoid sinus: a new classification. *Neurosurgery* 2010;66(4):797–816.
31. Delano MC, Fun FY, Zinreich SJ. Relationship of the optic nerve to the posterior paranasal sinuses: a CT anatomic study. *Am* 1996;17(4):669–75.
32. O’Brien WT, Sr., Hamelin S and Weitzel EK, The Preoperative Sinus CT: Avoiding a “CLOSE” Call with Surgical Complications. *Radiology* 2016;281(1):10–21. doi:10.1148/radiol.2016152230.